Manuscript Details

Manuscript number	GEODER_2018_52
Title	Relating soil C and organic matter fractions to structural stability
Article type	Research Paper

Abstract

Soil organic matter (SOM) is important for maintaining soil structural stability (SSS). The influence of soil organic carbon (SOC) and different organic matter components on various SSS measures were quantified. We used a silt loam soil with a wide range of SOC (0.0080-0.0427 kg kg-1 minerals) sampled in spring 2015 from the Highfield Ley-Arable Long-Term Experiment at Rothamsted Research. Four treatments were sampled: Bare fallow, continuous arable rotation, ley-arable rotation, and grass. Soils were tested for clay dispersibility (DispClay), clay-SOM disintegration (DI, the ratio between clay content without and with SOM removal) and dispersion of particles <20 μm. The SSS tests were related to SOC, permanganate oxidizable carbon (POXC), hot water-extractable carbon (HWC), mid-infrared photoacoustic spectroscopy (FTIR-PAS) and mineral fines/SOC ratio. SSS increased with increasing content of SOM components. The relationships between SOM components and SSS followed a broken-stick regression with a change point at ~0.0230 kg SOC kg-1 minerals (clay/SOC~10) coinciding with a change from the tilled treatments to the grass treatment. We found a greater influence of SOC, POXC and HWC on SSS at contents below the change point than above. A stronger linear relation between POXC and DispClay compared to SOC and HWC suggests that POXC was a better predictor of the variation in DispClay. POXC and HWC were less related to DI than SOC. The grass treatment had a very stable structure, shown in all SSS tests, probably due to the absence of tillage and large annual inputs of stabilizing agents. This suggests that a change in management from arable rotation to permanent grass is an effective tool for improving SSS.

Keywords	soil structural stability; soil organic carbon; permanganate oxidizable carbon; hot water-extractable carbon; soil management
Corresponding Author	Johannes Lund Jensen
Corresponding Author's Institution	Aarhus University - Department of Agroecology
Order of Authors	Johannes Lund Jensen, Per Schjønning, chris chris.watts@rothamsted.ac.uk, Bent T. Christensen, Clément Peltre, Lars Munkholm
Suggested reviewers	Mike Beare, Hugh Riley, Denis Angers, Cassio Antonio Tormena, Pascal Boivin

Submission Files Included in this PDF

File Name [File Type]

Cover_Letter.docx [Cover Letter]

Highlights.docx [Highlights]

Manuscript.docx [Manuscript File]

Appendix A. Supplementary figures.docx [e-Component]

To view all the submission files, including those not included in the PDF, click on the manuscript title on your EVISE Homepage, then click 'Download zip file'.

Johannes Lund Jensen
PhD Student
Soil Physics and Hydropedology
Dept. of Agroecology
Faculty of Science and Technology
Aarhus University
Blichers Allé 20
DK-8830 Tjele, Denmark

Mobile: +45 2636 0847
jlj@agro.au.dk
http://agro.au.dk/en/research/sektioner/soil-physics-and-hydropedology/

AARHUS
UNIVERSITY

January 18th, 2018

To the Editorial Board of *Geoderma*,

Please consider the attached manuscript entitled "**Relating soil C and organic matter fractions to structural stability**" by Jensen et al. for review and publication in *Geoderma*. It describes original research not published elsewhere and not submitted for publication in other journals.

Soil organic matter (SOM) is important for maintaining soil structural stability (SSS).The current study relates a number of SOM components to various SSS tests using contrasting treatments from the Highfield Ley-Arable Long-Term Experiment at Rothamsted Research (UK). This was done without confounding effects of soil type, soil texture, and climate. The results showed that the relationships between SOM components and SSS followed a broken-stick regression with a change point coinciding with a change from the tilled treatments to the grass treatment. The effect of increasing SOM components on SSS was greater below the change point, i.e. at low contents. The grass treatment had a very stable structure indicating that changing management from arable rotation to permanent grass is an effective tool for improving SSS.

If you have any further questions regarding our manuscript submission, please do not hesitate to contact me.

Sincerely,
Johannes Lund Jensen

Highlights

- Soil structural stability increased with an increase in SOM components

- The effect of increasing SOM components was greater at low contents

- The change point for soil structural stability was at a clay/SOC ratio close to 10

- Grassland soil has a very stable structure compared to tilled soil

1   Relating soil C and organic matter fractions to structural stability

2

3   Johannes L. Jensen[*1], Per Schjønning[1], Christopher W. Watts[2], Bent T. Christensen[1], Clément

4   Peltre[3], Lars J. Munkholm[1]

5

6   [1] Department of Agroecology, Aarhus University, Blichers Allé 20, 8830 Tjele, Denmark

7   [2] Department of Sustainable Agriculture Sciences, Rothamsted Research, Harpenden, Hertfordshire

8   AL5 2JQ, United Kingdom

9   [3] Department of Plant and Environmental Sciences, University of Copenhagen, Thorvaldsensvej 40,

10   1821 Frederiksberg, Denmark

11   [*] Corresponding author

12   *E-mail address*: jlj@agro.au.dk (J. L. Jensen).

13

14   Type of Paper: Original research paper

15   Number of figures: 6

16   Number of tables: 3

1

ABSTRACT

Soil organic matter (SOM) is important for maintaining soil structural stability (SSS). The influence of soil organic carbon (SOC) and different organic matter components on various SSS measures were quantified. We used a silt loam soil with a wide range of SOC (0.0080-0.0427 kg kg^{-1} minerals) sampled in spring 2015 from the Highfield Ley-Arable Long-Term Experiment at Rothamsted Research. Four treatments were sampled: Bare fallow, continuous arable rotation, ley-arable rotation, and grass. Soils were tested for clay dispersibility (DispClay), clay-SOM disintegration (DI, the ratio between clay content without and with SOM removal) and dispersion of particles <20 µm. The SSS tests were related to SOC, permanganate oxidizable carbon (POXC), hot water-extractable carbon (HWC), mid-infrared photoacoustic spectroscopy (FTIR-PAS) and mineral fines/SOC ratio. SSS increased with increasing content of SOM components. The relationships between SOM components and SSS followed a broken-stick regression with a change point at ~0.0230 kg SOC kg^{-1} minerals (clay/SOC~10) coinciding with a change from the tilled treatments to the grass treatment. We found a greater influence of SOC, POXC and HWC on SSS at contents below the change point than above. A stronger linear relation between POXC and DispClay compared to SOC and HWC suggests that POXC was a better predictor of the variation in DispClay. POXC and HWC were less related to DI than SOC. The grass treatment had a very stable structure, shown in all SSS tests, probably due to the absence of tillage and large annual inputs of stabilizing agents. This suggests that a change in management from arable rotation to permanent grass is an effective tool for improving SSS.

Keywords: soil structural stability; soil organic carbon; permanganate oxidizable carbon; hot water-extractable carbon; soil management

41 **Abbreviation**: A, Continuous arable rotation; BF, Bare fallow; CEC, Cation exchange capacity; DI,

42 Clay-SOM disintegration; DispClay, Clay dispersibility; DispFines20, Dispersion of particles <20

43 μm; Fines20, Mineral particles <20 μm; FTIR-PAS, Mid-infrared photoacoustic spectroscopy; G,

44 Grass; HWC, Hot water-extractable carbon; LA, Ley-arable rotation; LF-free-SOC, Light fraction-

45 free-SOC; LFSOC, Light fraction organic carbon; NTU, Nephelometric turbidity unit; PCA,

46 Principal component analysis; POXC, Permanganate oxidizable carbon; SSA, Specific surface area;

47 SSS, Soil structural stability.

1. Introduction

The importance of soil organic matter (SOM) on key soil properties and functions is well-known (e.g., Johnston et al., 2009), and as a consequence loss of SOM is considered as a major threat to sustained soil functions (Amundson et al., 2015). One soil property affecting key soil functions is soil structure. Soil structure is the relative arrangement of particles and pores (Dexter, 1988), and the ability of soil structure to resist external stresses both mechanical and or from water is soil structural stability (SSS). Greater SSS is essential for minimizing the risk of downward transport of fine particles carrying pollutants to the water environment (de Jonge et al., 2004), soil erosion (Le Bissonnais, 1996), soil cementing and seedbeds with hard and non-friable aggregates (Kay and Munkholm, 2004). SOM content is an important factor affecting SSS (Bronick and Lal, 2005), and a range of studies have shown that an increase in SOM content increases SSS (e.g., Jensen et al., 2017a; Watts and Dexter, 1997).

Soil organic carbon (SOC) is the main constituent of SOM and since an increase in SOC content generally increases SSS it may serve as a proxy for SSS. Labile organic compounds are considered readily decomposable, and are potentially better indicators for soil functions (Haynes, 2005). For example, permanganate oxidizable carbon (POXC) is considered a processed labile component of SOM and has been found to be more sensitive to differences in management than total SOC (Culman et al., 2012). POXC is easy and cheap to measure, and has been suggested as the best single predictor of soil health (Fine et al., 2017) and as a better predictor of crop productivity than total SOC (Hurisso et al., 2016). Similarly, hot water-extractable carbon (HWC) has been highlighted as a soil quality indicator more sensitive to management changes than total SOC (Ghani et al., 2003). HWC is considered a labile component of SOM consisting of microbial and plant derived material (Hirsch et al., 2017; Villada et al., 2016). Another measure, which potentially could better explain changes in SSS than total SOC could be to subtract light fraction organic

4

72 carbon (LFSOC) from total SOC since LFSOC is a fraction not closely associated to mineral

73 particles (Gregorich et al., 2006). Mid-infrared photoacoustic spectroscopy (FTIR-PAS) can be used

74 to assess differences in SOM quality (Peltre et al., 2014; Peltre et al., 2017), which potentially could

75 improve the explanatory power in predicting SSS.

76   Increasing evidence suggest that soils exhibit a capacity factor for carbon sequestration also

77 known as saturation state (Hassink, 1997; McNally et al., 2017). The saturation state of the soil has

78 been found to influence the SSS measure, clay dispersibility, rather than SOC *per se* (Dexter et al.,

79 2008). The saturation state has been assessed through the clay/SOC ratio, and a critical value close

80 to 10 corresponding to a soil where the mineral particles are saturated with SOC has been found in

81 several studies (Dexter et al., 2008; Getahun et al., 2016; Jensen et al., 2017a; Schjønning et al.,

82 2012). Soils with clay/SOC>10 may thus be considered SOC-unsaturated, and for such soils SSS

83 may be reduced. A similar threshold has been found for mineral particles <20 μm (Fines20) where

84 the ratio of Fines20/SOC>20 indicates less SSS. Consequently, these mineral fines to SOC ratios

85 may serve as soil type independent threshold values for SSS.

86   Previous studies often rely on samples retrieved from contrasting sites with different soil

87 types and textures making quantification of the effect of SOM components on SSS dubious. This

88 because the effects on SSS can be affected by other aggregate forming factors. More knowledge on

89 the quantitative importance of SOM components on SSS using different pretreatments and energy

90 input in the tests are needed.

91   The objective of this study was to quantify the influence of SOC on soil structural stability

92 parameters determined in different ways and to test if knowledge about SOM characteristics could

93 improve the predictive ability. A wide range of measures for the determination of SSS exists

94 ranging in sample preparation, pretreatment, degree of disturbance and quantification (Le

95 Bissonnais, 1996; Pojasok and Kay, 1990; Pulido Moncada et al., 2015). In this study, we applied

96 stability tests varying in pretreatment and ranging from low to very high degree of disturbance for a

97 comprehensive evaluation of SOC effects on SSS. Soil was retrieved from the Highfield Ley-Arable

98 Long-Term Experiment at Rothamsted Research (Highfield-LTE), a silt loam with a relatively

99 homogeneous topsoil texture and a large gradient in SOC that has developed during at least 56 years

100 of contrasting management practices without the confounding effects of soil type, soil texture and

101 climate. Treatments were selected to obtain the widest possible gradient in SOC content, and thus

102 ensuring major differences in SOM components.

103

104 **2. Materials and methods**

105 *2.1 The Highfield-LTE and treatments*

106   The Highfield-LTE was established in 1949 on a silt loam soil (Table 1) at Rothamsted

107 Research, Harpenden, UK (51°80'N, 00°36'W) in a field that had been under permanent grass for

108 centuries. The soil belongs to the Batcombe series, and the parent material include a relatively silty

109 (loess-containing) superficial deposit overlying and mixed with clay-with-flints (Avery and Catt,

110 1995). The soil is classified as an Aquic Paludalf (USDA Soil Taxonomy System) and Chromic

111 Luvisol (WRB) (Watts and Dexter, 1997). Average annual temperature and precipitation are 10.2ºC

112 (mean of 1992-2014) and 718 mm (mean of 1981-2010), respectively (Scott et al., 2014).

113   We selected three treatments in the ley-arable experiment:

114 Continuous arable rotation (A), winter cereals (winter wheat, *Triticum aestivum* L. and winter oats,

115 *Avena sativa* L.) fertilized with 220 kg N ha^{-1} y^{-1} and maintained under standard Rothamsted farm

116 practice with straw removed. Ley-arable rotation (LA), three-year grass/clover ley (meadow fescue,

117 *Festuca pratensis* L.; timothy-grass, *Phleum pratense* L.; white clover, *Trifolium repens* L.)

118 followed by three years arable (managed as A). The grass/clover ley received no N and was cut and

6

119   removed in early summer. The small amount of regrowth was topped in early autumn and left on

120   the plots. Two of the sampled plots were drilled with winter cereals following three years of

121   grass/clover, whereas the other two were drilled with grass/clover following three years of winter

122   cereals. Grass (G), ploughed and reseeded to grass (predominantly rye grass, *Lolium perenne* L.)

123   when the experiment was established (1949). The grass was managed as the grass/clover ley in LA.

124   We also selected the bare fallow (BF) treatment, which is not part of the original ley-arable

125   experiment and located adjacent to the ley-arable experiment (denoted Highfield bare fallow and

126   Geescroft bare fallow). The BF treatment has been maintained free of plants by regular tillage

127   (ploughed or rotavated two to four times a year) since 1959. The ploughing depth in BF, A and LA

128   was 0.23 m. The A, LA and G plots were fertilized with 65 kg P ha^{-1} and 250 kg K ha^{-1} every three

129   years.

130   The A, LA and G treatments were part of a randomized block design with four field

131   replicates, whereas the four BF plots were located at one end of the experiment (Fig. 1). The

132   dimensions of the LA plots were 50 m x 7 m, whereas it was 10 m x 6 m for the other plots. The A,

133   LA and G plots were smaller since they were part of a reversion experiment initiated in 2008. For

134   more details see Johnston (1972) and the electronic Rothamsted Archive

135   (www.era.rothamsted.ac.uk).

136   *2.2 Soil sampling*

137   Soil was sampled in March 2015 at field capacity water conditions (corresponding

138   approximately to a soil water potential of -100 hPa). Soil blocks (2750 cm^3) were sampled from the

139   6-15-cm soil layer by careful use of a spade. Three sampling sites in each experimental plot were

140   randomly chosen and labeled subplot. One of these blocks was extracted from each subplot adding

141   up to three blocks per plot. The soil was kept in rigid containers to prevent soil disturbance during

142   transport and stored in a field-moist condition at 2ºC until required. Soil from the blocks at subplot

7

143 level were spread out in steel trays at room temperature, carefully fragmented by hand in several

144 sittings along natural planes of weakness and finally left to air-dry.

2.3 Basic chemical and physical analysis

146   Soil texture of air-dried bulk soil (crushed and passed through a 2-mm sieve) was determined

147 by the hydrometer method for clay (<2 μm) and silt (2-20 μm) content and the sieve method for

148 mineral particles >63 μm (Gee and Or, 2002). The soil was tested for $CaCO_3$ by adding a few

149 droplets of 10% HCl, but none was found. SOM was removed by H_2O_2 before estimation of clay

150 and silt as described in Jensen et al. (2017b). The SOC content was determined on ball-milled

151 subsamples using dry combustion (Thermo Flash 2000 NC Soil Analyzer, Thermo Fisher Scientific,

152 Waltham Massachusetts, USA). Specific surface area (SSA) was determined by the ethylene glycol

153 monoethyl ether method (Petersen et al., 1996), and cation exchange capacity (CEC) was

154 determined after Kalra and Maynard (1991). Soil pH was determined in 0.01 M calcium chloride

155 ($CaCl_2$) solution (1:2.5, *w*/w). Clay, silt and SOC content were determined at subplot level, whereas

156 the other properties were determined at plot level.

2.4 Soil organic matter characteristics

158   Permanganate oxidizable carbon (POXC) was determined at subplot level following Culman

159 et al. (2012). Air-dry 2-mm sieved soil equivalent to 2.5 g oven-dry weight was weighed into a 50

160 ml falcon tube, and was shaken in 18.0 ml of distilled water and 2.0 ml 0.2 M potassium

161 permanganate ($KMnO_4$) with pH 7.2 at 33 rpm for 2 min. After shaking, the soil was allowed to

162 settle for 10 min after which 0.5 ml of the supernatant was transferred to falcon tubes containing

163 49.5 ml of water. The absorbance of the diluted solution was measured at 550 nm using a

164 spectrophotometer (Thermo Electron Spectronic Helios Alpha Beta UV-visible). Absorbance of

165   four standard stock $KMnO_4$ solutions were measured to create a standard curve, and the absorbance

166   of the samples were converted to POXC using the equation of Weil et al. (2003).

167   Hot water-extractable carbon (HWC) was determined at subplot level following Ghani et al.

168   (2003). Briefly, air-dry 2-mm sieved soil equivalent to 3 g oven-dry weight was weighed into a 50

169   ml falcon tube, and was shaken in 30 ml distilled water at 33 rpm for 30 min, at 20ºC. After

170   centrifugation (3500 rpm, 20 min) the supernatant was decanted, soil resuspended and shaken for 16

171   h at 200 rpm, at 80ºC. After centrifugation, the supernatant was transferred to 50 ml maxi-spin filter

172   tubes equipped with a cellulose acetate membrane filter (0.45 μm pore size), filtered by

173   centrifugation for 10 min at 3000 rpm and carbon determined by wet oxidation using a Shimadzu

174   TOC-V analyzer.

175   Fractionation based on density was determined at subplot level using a modification of the

176   method described by Sohi et al. (2001). Briefly, 10 g of air-dried 2-mm sieved soil was weighed

177   into a 50 ml falcon tube, 35 mL of NaI solution with a density of 1.8 g cm^{-3} was added, and the

178   solution was shaken at 33 rpm for 2 h. The suspension was centrifuged for 30 min after which

179   floating particles was transferred to a glass fiber filter (type GF/A, 110 mm diam., 1.6 μm retention,

180   Whatman International, Kent, UK), and filtered under suction in a vacuum filtration unit (Büchner

181   funnel). The light fraction organic matter (LFOM) retained on the filter was washed carefully and

182   transferred to a crucible. To ensure a quantitative removal of LFOM the procedure was repeated.

183   The remaining heavy fraction (HF) was washed three times and transferred to a large crucible. The

184   oven-dry weight of the LF and HF were estimated by drying (105 °C for 24 h). The amount of OM

185   recovered was estimated by loss-on-ignition (LOI; 500 °C for 4 h) both for the LFOM and HF. A 5

186   g air-dry bulk soil sample was dried to allow expressing results on an oven-dry basis after which

187   LOI was determined. The LOI of bulk soil was used to make a model to predict the SOC of the HF

188 based on a multiple regression of SOC against LOI and clay (Model H2.1, Table 2 in Jensen et al.,

189 2018):

190 SOC = 0.515 LOI (P<0.001) - 0.043 Clay (P<0.001), (n=48, R^2= 0.990)   (1)

191   Ten tests without soil (blind tests) were performed. The blind test estimate was subtracted

192 from the LFOM estimate. The LFOM was converted to LFSOC by multiplying with 0.515 (Eq. 1),

193 expressed as percentage of the sum of LFSOC and HFSOC, and normalized to the measured SOC

194 content. Light fraction-free-SOC (LF-free-SOC) was calculated by subtracting LFSOC from SOC.

195   Fourier transform mid-infrared photoacoustic spectroscopy (FTIR-PAS) was determined at

196 plot level following Peltre et al. (2014). Air-dry 2-mm sieved soil samples were ball-milled and

197 packed in 10-mm diameter cups and functional groups of soil components were investigated using a

198 Nicolet 6700 FTIR spectrometer (Thermo Scientific) equipped with a PA301 photoacoustic detector

199 (Gasera Ltd. Turku, Finland). Spectra were recorded with an average of 32 scans within the range

200 4000-600 cm^{-1} and with 2 cm^{-1} intervals. A flow of helium was used as purge gas to remove noise

201 produced by ambient moisture and CO_2 as well as moisture from the sample after insertion of the

202 cup in the photoacoustic detector chamber. We focused on the 1700-1300 cm^{-1} region to reduce

203 overlapping from bands arising from soil minerals. The spectral peak area between 3000 and 2800

204 cm^{-1} were integrated as described in Peltre et al. (2017), and reflects the amount of aliphatics in the

205 soil (Leifeld, 2006).

206 *2.5 Soil structural stability*

207   Clay dispersibility (DispClay) was determined at subplot level on 1-2 mm aggregates

208 extracted from the air-dry 2-mm sieved soil. The aggregates were adjusted to a matric water

209 potential of -100 hPa as described in Schjønning et al. (2012). In short, the aggregates were put on a

210   tension table at -100 hPa, gradually exposed to reduced suctions until -3 hPa, and finally

211   equilibrated at -100 hPa by gradually increased suctions. The rewetting was done with great caution

212   to avoid air explosion (slaking). Artificial rainwater was added to cylindrical plastic bottles

213   containing 10 g of aggregates in order to obtain a soil:water ratio of 1:8 by weight. After end-over-

214   end rotation (33 rpm, 23-cm diameter rotation) for 2 min, the bottles were left to stand for 230 min,

215   after which the upper 50 mm (60 ml) containing particles ≤ 2 μm was siphoned off. The weight of

216   dispersed clay was determined after oven-drying (105 °C for 24 h) and corrected for particles >250

217   μm isolated by chemical dispersion.

218   Dispersion of particles <20 μm (DispFines20) was measured at different time steps at plot

219   level on field-moist soil. Soil was retrieved from the minimally-disturbed soil cubes using a small

220   corer (22-mm diameter) and gently crumbled by hand to pass an 8-mm sieve. Artificial rainwater

221   was added to a cylindrical bottle containing soil equivalent to 1 g oven-dry weight to obtain a

222   soil:water ratio of 1:100 by weight. The bottle was end-over-end rotated (33 rpm, 23-cm diameter

223   rotation) for 2, 4, 8, 16, 32, 64 and 128 min. At each time step the bottle was left to stand for 67 sec,

224   after which the upper 30 ml containing particles <20 μm was siphoned off and turbidity of the

225   suspension was measured on a Hach 2100AN turbidimeter (Hach, Loveland, CO). After the

226   turbidity measurements taken at time steps 2-64 min the soil suspension was transferred back to the

227   bottle. Thus, the measurements at the different time steps was done on the same sample. After the

228   final measurement, the 30 ml was transferred to a beaker and bulked at treatment level. For each

229   treatment, correlations between nephelometric turbidity unit (NTU) and particle concentration were

230   made by doing dilution series. The calibration curves can be seen in Fig. S1 in Supplementary

231   material. The results were corrected for particles > 250 μm isolated by chemical dispersion.

232   Soil samples at subplot level were analyzed without H_2O_2-removal of SOM before estimation

233   of clay as described in Jensen et al. (2017b), and clay-SOM disintegration (DI) was calculated as

234   the ratio between clay content estimated without SOM removal and with removal. Soil with DI

235   values <1 kg kg^{-1} can be interpreted as extremely stable since they have resisted disintegration after

236   end-over-end rotation for 18 h in sodium pyrophosphate.

237   *2.6 Calculations and statistics*

238   The soil components measured in the paper are given as fractions of oven-dry weight (105ºC

239   for 24 h) of the SOM-free mineral fraction. This includes mineral particle size fractions, SOC,

240   POXC, HWC, LF-free-SOC, SSA, CEC and DispClay. DispFines20 is given as a fraction of SOM-

241   free mineral fraction <20 μm.

242   The statistical analysis and processing of spectral data applied the R-project software package

243   Version 3.4.0 (R Foundation for Statistical Computing). Treatment effects for the comparison of A,

244   LA and G were analyzed with a linear mixed model including block as a random effect. The

245   criterion used for statistical significance of treatment effects was $P<0.05$. When the treatment effect

246   was significant, further analyses were made to isolate differences between treatments (pairwise

247   comparisons) using the general linear hypotheses (*glht*) function implemented in the R *multcomp*

248   package and the Kenward-Roger method to calculate degrees of freedom (Kenward and Roger,

249   2009). Treatment differences for the comparison of BF and the other treatments were calculated

250   based on a pairwise *t*-test, acknowledging that this is a less robust test, and that the treatment

251   differences could be due to soil variation since the BF treatment is not a part of the ley-arable

252   experiment. Inverse transformation was performed on DispFines20 to stabilize the variance. The

253   broken-stick model was fitted using the *segmented* package in R. A piece-wise linear model was

254   used:

255     $$y = \beta_0 + \beta_1(x) + \beta_2(x-c)^+ + e \qquad\qquad (2)$$

256   where y is the dependent variable, x is the independent variable, c is the change point and e is the

257   residual standard error (Toms and Lesperance, 2003). The $^+$ sign indicates that the last term only is

258   valid when $x>c$.

259   Spectral data processing included baseline correction, smoothing using a Savitzky-Golay filter

260   calculated on three data points on each side with a zero-order polynomial, and normalization by the

261   average absorbance on the whole spectra. Principal component analysis (PCA) on the FTIR-PAS

262   spectra was performed using the *ade4* package in R.

263

264   **3. Results**

265   *3.1 Basic soil characteristics*

266   Differences in the contents of clay, silt and sand were in general not significant between

267   treatments (Table 1) and the effect of the contrasting management practices could be investigated

268   without confounding effects related to soil texture. SSA differed significantly following the same

269   pattern as SOC. CEC was significantly higher for G compared to the BF treatment, and the amount

270   of exchangeable Ca^{2+} was significantly higher for G compared to the other treatments. Soil pH was

271   not affected by the contrasting management practices.

272   *3.2 Soil organic matter characteristics*

273   Concentration of SOC differed significantly in the order G>LA=A>BF (Table 2). POXC,

274   HWC, LFSOC, and the aliphatic C-H peak area (3000-2800 cm^{-1}) followed the treatment

275   differences in SOC. The full spectral range as well as the SOM fingerprint region (1700-1300 cm^{-1})

276   at plot level can be seen in Supplementary material, Figs. S2 and S3, respectively.

277   The aliphatic peak area normalized by the SOC content was higher in the BF than the G

278   treatment indicating that SOM in G soil was more depleted in aliphatics. The POXC contributed to

279   1.7, 2.6, 2.8 and 2.5 % of total SOC, respectively, and the HWC in BF, A, LA and G contributed to

280   4.6, 4.5, 5.0 and 4.9 % of total SOC, respectively. The increase in POXC with an increase in SOC

281   was different for the G treatment compared to A and LA (Fig. 2a). The narrow range in SOC

282   content for BF did not allow an evaluation of the POXC-SOC relation within the SOC-depleted BF

283   soil, but the first slope of the broken-stick model was similar to a linear regression with only A and

284   LA (35.4 compared to 33.9 g kg^{-1} SOC). This indicates that the level of POXC for BF was in line

285   with the trend of the other tilled treatments (A and LA). The x-intercept of the broken-stick model

286   in Fig. 2a was 0.00458 kg SOC kg^{-1} minerals, and suggests that no POXC was oxidized at and

287   below this SOC content. For the wide range in SOC in this study, HWC correlated linearly to SOC

288   with an intercept value close to zero (Fig. 2b). Our data thus point to a concentration of ~0.05 kg

289   HWC per kg SOC (~5%) irrespective of SOC level.

290   The PCA analysis based on the 1700-1300 cm^{-1} region clearly separated the treatments on the

291   first principal component (PC1) explaining 84.6% of the spectral variance (Fig. 3a). Field plots

292   from the G and BF treatment were located on the left and right side of the PCA plane, respectively.

293   Field plots from the A and LA treatments were in the center of the PCA plane and did not differ

294   much. Examination of the loading of PC1 indicated that BF soils were relatively enriched in organic

295   compounds vibrating in the range between 1700 and 1580 cm^{-1} with a peak at 1625 cm^{-1} (Fig. 3b).

296   Absorption in this region is attributed to vibration of aromatics and carboxylate at 1600-1570 cm^{-1},

297   amine at 1610 cm^{-1}, clay-bound water at 1640 cm^{-1}, aromatics at 1660-1600 cm^{-1} and amides at

298   1670-1640 cm^{-1} (Table 1 in Peltre et al., 2017). In contrast, G soils were relatively enriched in

299   organic compounds vibrating in the range between 1580-1495 cm^{-1} and 1475-1325 cm^{-1} with peaks

300   at 1550, 1510 and 1385 cm^{-1} (Fig. 3b). These regions are attributed to vibration of nitrate at 1380

14

301 cm^{-1}, carboxylate at 1390 cm^{-1}, amide III at 1420 cm^{-1}, carbonates at 1430 cm^{-1}, aliphatic methyls at

302 1445-1350 cm^{-1}, lignin rings at 1505-1515 cm^{-1} and amide II at 1570-1540 cm^{-1} (Table 1 in Peltre et

303 al., 2017).

3.3 Soil structural stability

305 The amount of dispersible clay differed significantly in the order BF>A>LA>G, and the

306 disintegration of soil without SOM removal was significantly lower for the G treatment compared

307 to the other treatments (Table 2). Linear, semi-logarithmic and broken-stick models were employed

308 to describe the correlations of SOC, POXC and HWC to DispClay and DI (Table 3). The coefficient

309 of determination (R^2) was highest when DispClay and DI were related to SOC with a broken-stick

310 model (see relation on Fig. 4a). Similar relationships were found when relating POXC and HWC to

311 DispClay and DI (Figs. 4b and 4c).

312 Relating changes in DispClay to LF-free-SOC did not improve R^2 compared to SOC (Fig. 5a),

313 whereas LF-free-SOC increased the explained variation in DI by 1 %-unit (Fig. 5b).

314 DispFines20 was significantly lower for the G treatment compared to the other treatments at

315 all time steps (Fig. 6a), and the release-curve had a contrasting shape compared to the other

316 treatments. DispFines20 was significantly lower for the LA than the A treatment after both 64 and

317 128 min. The release rate was markedly higher in the beginning for BF, A and LA compared to G

318 (Fig. 6b). From approx. 24 min onwards, G had a higher release rate compared to the other

319 treatments. At all time steps, DispFines20 was virtually constant across the four G treatment plots

320 despite a range in SOC, while considerable variation was observed for the narrower SOC ranges of

321 the other three treatments (Fig. S4 in Supplementary material).

322

4. Discussion

4.1 Linking soil organic matter components to soil structural stability

POXC has been promoted as a relatively processed or stabilized pool of active SOC (Culman et al., 2012), and as organic material to support biological functions (Idowu et al., 2008), while HWC has been promoted as an indicator of soil biochemical quality (Ghani et al., 2003). Both SOM fractions are considered labile and sensitive indicators for assessing management-induced changes (Culman et al., 2012; Ghani et al., 2003). Labile organic compounds are known to bond mineral particles together and thus stabilize them against mechanical damage (Degens, 1997). However, this mechanism would not be expected to play any role for the clay-SOM disintegration (DI) test that involves a rather extreme disruptive energy to soil structural units (end-over-end shaking for 18 h in sodium pyrophosphate solution). In accordance with this, we note a higher coefficient of determination in the broken-stick regression relating DI to SOC (R^2=0.88) than for POXC and HWC (R^2=0.82 and R^2=0.79, respectively). One may speculate that stable organo-mineral associations (i.e. at submicro-aggregate and primary particle scale) are causing the extreme stability at high SOC contents. The similar pattern observed for POXC and HWC (broken-stick) then relates to the near linear relations observed between total SOC and these two fractions (Fig. 2).

For the DispClay SSS measure, we observe nearly identical coefficients of determination in the broken-stick models describing the data: R^2 equals 0.94, 0.93 and 0.91 with SOC, POXC and HWC as predictor (Table 3). We further note that the broken-stick is "less broken" especially when using POXC as predictor of trends in data (slope ratios, Table 3). This observation is supported by a higher ability of POXC to describe data in a linear model (R^2=0.91) compared to HWC and SOC (R^2=0.82 and R^2=0.84, respectively). Overall, this may indicate that POXC is superior to SOC and HWC in describing the variation in DispClay.

Our study does not allow a definite clarification regarding which mechanisms are in play in SSS. The indication that POXC is superior in describing the variation in DispClay may be related to

348 a link to bonding agents such as polysaccharides, which are assumed predominantly active at micro-

349 aggregate scale (Tisdall and Oades, 1982). However, the composition of POXC is unknown, which

350 is related to the destruction of the fraction by oxidization. The lower predictive ability of HWC to

351 explain SSS data and its close correlation to SOC may indicate that it is a too simplistic quality

352 characteristic of SOC. Other studies have emphasized the need to focus on the carbohydrate-C

353 contents in the hot water-extracts (e.g., Haynes, 2005), and studies have shown that hot water-

354 extractable carbohydrate-C was a better predictor of SSS than SOC (Haynes and Swift, 1990).

355   Changes in DispClay and DI may be better explained by LF-free-SOC than total SOC.

356 However, the difference in using LF-free-SOC compared to SOC was marginal (Fig. 5). The

357 decrease in DispClay and DI when going from BF to G could be related to a general enrichment in

358 aliphatics and lignin, and a decrease in carboxylic groups and amides (Table 2, Fig. 3). The higher

359 amount of carboxyl-rich and amide-rich SOM suggest that the SOM in the BF soils were more

360 oxidized being in agreement with the findings of Barré et al. (2016). Such compounds have been

361 related to microbial processed and stable SOM in organo-mineral associations (Kleber et al., 2015).

362 A higher proportion of aliphatics in SOM from the BF soils also support the presence of a more

363 decomposed SOM. The results indicate that plant residues were decomposed rapidly in the BF soils

364 leaving behind SOM enriched in microbial processed OM. In contrast, less oxidized and continually

365 renewed compounds accumulated in the G soils.

366 *4.2 Management system effects on soil structural stability*

367   The four treatments can be seen as three management systems comprising the BF treatment

368 with intensive tillage, no plants or carbon input, the A and LA treatments with plants and tillage,

369 and the G treatment with plants and absence of tillage. The G treatment differed from the other

370 treatments by having a very stable structure and a better ability to resist increasing degrees of

371 disturbance. Consequently, the potential maximum SSS was only fully achieved for the long-term G

372 treatment. This was reflected in the DispClay and DI tests where the change point of the broken-

373 stick model for SOC content was confounded with treatment, and represented a change from the LA

374 to G treatment (Fig. 4a). Also the results on DispFines20 support a change in stability between the

375 G treatment and the other treatments illustrated by the contrasting curve, release rate and higher

376 stability at all time steps (Fig. 6). Permanent grass stands out from the other treatments by having a

377 greater input of above- and belowground plant residues. Hirsch et al. (2009, 2017) found a

378 markedly greater number of roots and mesofauna in G compared to BF and A, and a larger

379 abundance of fungi. Roots and fungal hyphae can act as binding agents, enmesh aggregates

380 (Elmholt et al., 2008; Tisdall and Oades, 1982), and potentially increase SSS, and mesofauna can

381 contribute to stability via stabilizing decomposition products (Oades, 1993). In addition, the effect

382 of these stabilizing agents are persistent since they are continuously replaced, and remain

383 undisturbed due to the absence of tillage. The limited effect of SOC on DispFines20 within the G

384 treatment at all time steps (Fig. S4 in Supplementary material) may be related to the larger scale

385 applied in the test, i.e. whole-soil samples not broken down to more than 8 mm. At a larger scale,

386 management system drivers such as macro-aggregate stabilizing agents seemed to be more distinct,

387 while SOC played a minor role. The greater stability of the G treatment may also be related to the

388 absence of tillage shown to be detrimental to the preservation of stabilizing agents.

389 The higher amount of soluble Ca^{2+} ions in the G treatment increases the tendency of clay

390 particles to flocculate (Le Bissonnais, 1996), and may also contribute to the higher stability.

391 However, the importance of cations for aggregate stability is considered less important in soil high

392 in clay or SOC (Bronick and Lal, 2005). Matthews et al. (2008) found a decrease in wettability for

393   G, whereas wettability was similar for BF, A and LA treatments. Thus, the very stable structure of

394   the G soil may also be partially related to decreased wettability.

395   *4.3 Critical carbon levels*

396   Our SSS measures DI and DispClay showed a change in the relation to SOC at around 0.0230

397   kg kg^{-1} minerals for this soil (broken-stick change point; Fig. 4a). The carbon saturation concept

398   (Six et al., 2002; Stewart et al., 2007) implies the existence of a SOC concentration that for a given

399   soil provides a full "coverage" of the surface of soil minerals with SOC. This potential carbon

400   storage capacity (Ingram and Fernandes, 2001) was verified for a range of grassland soils assumed

401   saturated with organic carbon (Hassink, 1997). A SOC concentration of ~0.0230 kg kg^{-1} minerals

402   found in this study may thus be hypothesized to reflect the potential storage capacity for this soil.

403   The broken-stick pattern for DispClay indicates that SOC influences SSS more for soils with SOC

404   below the change point than above (Fig. 4a). DispClay increases more with reduction in SOC when

405   the soil is unsaturated with carbon (below the change point) than when it is saturated. This is in line

406   with Jensen et al. (2017a), who found SOC to be important for SSS for SOM-depleted soil.

407   Interestingly, the DI test with extreme energy input showed that all unsaturated soil samples

408   behaved similarly and fully disintegrate (slope not significantly different from zero; Fig. 4a).

409   The SOC threshold for a change in SOC effects on SSS differ from soil to soil, e.g. around

410   0.0110 kg SOC kg^{-1} minerals for a sandy loam in Denmark (Jensen et al., 2017a). Thus, SOC

411   critical to SSS seems soil type dependent. Dexter et al. (2008) and Jensen et al. (2017a) found an

412   increasingly compromised SSS when the clay/SOC ratio was above 10. Schjønning et al. (2012)

413   and Jensen et al. (2017a) found that a Fines20/SOC ratio of 20 serve as a similar critical threshold

414   value. The clay/SOC and Fines20/SOC ratios for a change in DispClay and DI were calculated by

415   dividing the average clay or Fines20 content with the change point giving values of 11 and 23,

416 respectively. Thus, our results support the soil clay/SOC~10 or Fines20/SOC~20 as defining factors

417 for SSS.

418   In this study the thresholds for changes in SOC (as well as POXC and HWC) effects on SSS

419 is confounded with management (Fig. 4). Thus the calculated soil mineral fines/SOC thresholds

420 may relate to a quantity of SOC as well as management system (as discussed in section 4.2). This

421 was unavoidable since systems with a wide range in SOC often will require contrasting

422 management. However, confounding effects derived from differences in soil type, soil texture and

423 climate were eliminated.

424

425 **5. Conclusions**

426   We exploited the unique range in SOM within Highfield, which has developed due to

427 contrasting long-term management practices. Soil structural stability (SSS) increased with an

428 increase in SOM components. However, the relationships followed a broken-stick regression with

429 the greater effect occurring when SOM components were less. The SOM fractions permanganate

430 oxidizable carbon (POXC) and hot water-extractable carbon (HWC) were less related to clay-SOM

431 disintegration than SOC. However, POXC seemed superior in describing the variation in clay

432 dispersibility compared to SOC and HWC. The permanent grass had a very stable structure - even

433 when exposed to high degree of disturbance. This may be ascribed to the management system,

434 which result in higher amount of stabilizing agents due to greater and annually renewed inputs of

435 above- and belowground plant residues as well as absence of tillage. Both aspects promote a high

436 abundance of soil microbiota and mesofauna. For this soil, management changes promoting SOM

437 content increased SSS up to a specific threshold coinciding with a change to permanent grass.

438 Consequently, increasing the SOC content at low contents or changing management from arable

20

439 rotation to permanent grass seem promising tools for improving SSS. Further, this study supports

440 the existence of critical soil mineral fines/SOC ratios for SSS with change points at clay/SOC~10

441 and Fines20/SOC~20.

442

457

458

459 **References**

460 Amundson, R., Berhe, A.A., Hopmans, J.W., Olson, C., Sztein, A.E., Sparks, D.L., 2015. Soil and

461   human security in the 21st century. Science 348, 1261071.

462 Avery, B.W., Catt, J.A., 1995. The soils at Rothamsted. Lawes Agricultural Trust, 1-44.

463 Barré, P., Plante, A.F., Cécillon, L., Lutfalla, S., Baudin, F., Bernard, S., Christensen, B.T., Eglin,

464   T., Fernandez, J.M., Houot, S., Kätterer, T., Le Guillou, C., Macdonald, A., van Oort, F.,

465   Chenu, C., 2016. The energetic and chemical signatures of persistent soil organic matter.

466   Biogeochemistry 130, 1-12.

467 Bronick, C.J., Lal, R., 2005. Soil structure and management: a review. Geoderma 124, 3-22.

468 Culman, S.W., Snapp, S.S., Freeman, M.A., Schipanski, M.E., Beniston, J., Lal, R., Drinkwater,

469   L.E., Franzluebbers, A.J., Glover, J.D., Grandy, A.S., Lee, J., Six, J., Maul, J.E., Mirksy,

470   S.B., Spargo, J.T., Wander, M.M., 2012. Permanganate Oxidizable Carbon Reflects a

471   Processed Soil Fraction that is Sensitive to Management. Soil Sci. Soc. Am. J. 76, 494-504.

472 de Jonge, L.W., Kjaergaard, C., Moldrup, P., 2004. Colloids and Colloid-Facilitated Transport of

473   Contaminants in Soils. Vadose Zone J. 3, 321-325.

474 Degens, B.P., 1997. Macro-aggregation of soils by biological bonding and binding mechanisms and

475   the factors affecting these: a review. Aust. J. Soil Res. 35, 431-460.

476 Dexter, A., Richard, G., Arrouays, D., Czyż, E., Jolivet, C., Duval, O., 2008. Complexed organic

477   matter controls soil physical properties. Geoderma 144, 620-627.

478 Dexter, A.R., 1988. Advances in characterization of soil structure. Soil Tillage Res. 11, 199-238.

479 Elmholt, S., Schjønning, P., Munkholm, L.J., Debosz, K., 2008. Soil management effects on

480   aggregate stability and biological binding. Geoderma 144, 455-467.

481 Fine, A.K., van Es, H.M., Schindelbeck, R.R., 2017. Statistics, Scoring Functions, and Regional

482   Analysis of a Comprehensive Soil Health Database. Soil Sci. Soc. Am. J. 81, 589-601.

483   Gee, G.W., Or, D., 2002. Particle-size analysis. In: J.H. Dane, G.C. Topp (Eds.), Methods of Soil

484   Analysis. Part 4 - Physical methods, Soil Science Society of America, Inc. Madison,

485   Wisconsin, USA, 255-294.

486   Getahun, G.T., Munkholm, L.J., Schjønning, P., 2016. The influence of clay-to-carbon ratio on soil

487   physical properties in a humid sandy loam soil with contrasting tillage and residue

488   management. Geoderma 264, Part A, 94-102.

489   Ghani, A., Dexter, M., Perrott, K.W., 2003. Hot-water extractable carbon in soils: a sensitive

490   measurement for determining impacts of fertilisation, grazing and cultivation. Soil Biol.

491   Biochem. 35, 1231-1243.

492   Gregorich, E.G., Beare, M.H., McKim, U.F., Skjemstad, J.O., 2006. Chemical and Biological

493   Characteristics of Physically Uncomplexed Organic Matter. Soil Sci. Soc. Am. J. 70, 975-

494   985.

495   Hassink, J., 1997. The capacity of soils to preserve organic C and N by their association with clay

496   and silt particles. Plant Soil 191, 77-87.

497   Haynes, R.J., 2005. Labile Organic Matter Fractions as Central Components of the Quality of

498   Agricultural Soils: An Overview. Adv. Agron. 85, 221-268.

499   Haynes, R.J., Swift, R.S., 1990. Stability of soil aggregates in relation to organic constituents and

500   soil water content. J. Soil Sci. 41, 73-83.

501   Hirsch, P.R., Gilliam, L.M., Sohi, S.P., Williams, J.K., Clark, I.M., Murray, P.J., 2009. Starving the

502   soil of plant inputs for 50 years reduces abundance but not diversity of soil bacterial

503   communities. Soil Biol. Biochem. 41, 2021-2024.

504   Hirsch, P.R., Jhurreea, D., Williams, J.K., Murray, P.J., Scott, T., Misselbrook, T.H., Goulding,

505   K.W.T., Clark, I.M., 2017. Soil resilience and recovery: rapid community responses to

506   management changes. Plant Soil 412, 283-297.

507   Hurisso, T.T., Culman, S.W., Horwath, W.R., Wade, J., Cass, D., Beniston, J.W., Bowles, T.M.,

508   Grandy, A.S., Franzluebbers, A.J., Schipanski, M.E., Lucas, S.T., Ugarte, C.M., 2016.

509   Comparison of Permanganate-Oxidizable Carbon and Mineralizable Carbon for Assessment

510   of Organic Matter Stabilization and Mineralization. Soil Sci. Soc. Am. J. 80, 1352-1364.

511   Idowu, O.J., van Es, H.M., Abawi, G.S., Wolfe, D.W., Ball, J.I., Gugino, B.K., Moebius, B.N.,

512   Schindelbeck, R.R., Bilgili, A.V., 2008. Farmer-oriented assessment of soil quality using

513   field, laboratory, and VNIR spectroscopy methods. Plant Soil 307, 243-253.

514   Ingram, J.S.I., Fernandes, E.C.M., 2001. Managing carbon sequestration in soils: concepts and

515   terminology. Agr. Ecosyst. Environ. 87, 111-117.

516   Jensen, J.L., Christensen, B.T., Schjønning, P., Watts, C.W., Munkholm, L.J., 2018. Converting

517   loss-on-ignition to organic carbon content in arable topsoil: Pitfalls and proposed procedure.

518   Eur. J. Soil Sci. (revised version submitted).

519   Jensen, J.L., Schjønning, P., Christensen, B.T., Munkholm, L.J., 2017a. Suboptimal fertilisation

520   compromises soil physical properties of a hard-setting sandy loam. Soil Res. 55, 332-340.

521   Jensen, J.L., Schjønning, P., Watts, C.W., Christensen, B.T., Munkholm, L.J., 2017b. Soil texture

522   analysis revisited: Removal of organic matter matters more than ever. PLOS ONE 12,

523   e0178039.

524   Johnston, A.E., 1972. The effect of ley and arable cropping systems on the amount of soil organic

525   matter in Rothamsted and Woburn Ley-Arable experiments. Report Rothamsted

526   Experimental Station for 1972, Part 2, 131-152.

527   Johnston, A.E., Poulton, P.R., Coleman, K., 2009. Chapter 1 Soil Organic Matter: Its Importance in

528   Sustainable Agriculture and Carbon Dioxide Fluxes. Adv. Agron. 101, 1-57.

529   Kalra, Y.P., Maynard, D.G., 1991. Methods manual for forest soil and plant analysis. Northern

530   Forestry Centre, Edmonton, Alberta.

531 Kay, B.D., Munkholm, L.J., 2004. Management-induced soil structure degradation - organic matter

532   depletion and tillage. In: P. Schjønning, S. Elmholt, B.T. Christensen (Eds.), Managing Soil

533   Quality: Challenges in Modern Agriculture. CABI Publishing, Wallingford, UK, 185-197.

534 Kenward, M.G., Roger, J.H., 2009. An improved approximation to the precision of fixed effects

535   from restricted maximum likelihood. Comput. Stat. Data An. 53, 2583-2595.

536 Kleber, M., Eusterhues, K., Keiluweit, M., Mikutta, C., Mikutta, R., Nico, P.S., 2015. Mineral–

537   Organic Associations: Formation, Properties, and Relevance in Soil Environments. Adv.

538   Agron. 130, 1-140.

539 Le Bissonnais, Y., 1996. Aggregate stability and assessment of soil crustability and erodibility: I.

540   Theory and methodology. Eur. J. Soil Sci. 47, 425-437.

541 Leifeld, J., 2006. Application of diffuse reflectance FT-IR spectroscopy and partial least-squares

542   regression to predict NMR properties of soil organic matter. Eur. J. Soil Sci. 57, 846-857.

543 Matthews, G.P., Watts, C.W., Powlson, D.S., Price, J.C., Whalley, W.R., 2008. Wetting of

544   agricultural soil measured by a simplified capillary rise technique. Eur. J. Soil Sci. 59, 817-

545   823.

546 McNally, S.R., Beare, M.H., Curtin, D., Meenken, E.D., Kelliher, F.M., Calvelo Pereira, R., Shen,

547   Q., Baldock, J., 2017. Soil carbon sequestration potential of permanent pasture and

548   continuous cropping soils in New Zealand. Glob. Change Biol. 23, 4544-4555.

549 Oades, J.M., 1993. The role of biology in the formation, stabilization and degradation of soil

550   structure. Geoderma 56, 377-400.

551 Peltre, C., Bruun, S., Du, C., Thomsen, I.K., Jensen, L.S., 2014. Assessing soil constituents and

552   labile soil organic carbon by mid-infrared photoacoustic spectroscopy. Soil Biol. Biochem.

553   77, 41-50.

554 Peltre, C., Gregorich, E.G., Bruun, S., Jensen, L.S., Magid, J., 2017. Repeated application of

555   organic waste affects soil organic matter composition: Evidence from thermal analysis,

556   FTIR-PAS, amino sugars and lignin biomarkers. Soil Biol. Biochem. 104, 117-127.

557 Petersen, L.W., Moldrup, P., Jacobsen, O.H., Rolston, D.E., 1996. Relations between specific

558   surface area and soil physical and chemical properties. Soil Sci. 161, 9-21.

559 Pojasok, T., Kay, B.D., 1990. Assessment of a combination of wet sieving and turbidimetry to

560   characterize the structural stability of moist aggregates. Can. J. Soil Sci. 70, 33-42.

561 Pulido Moncada, M., Gabriels, D., Cornelis, W., Lobo, D., 2015. Comparing Aggregate Stability

562   Tests for Soil Physical Quality Indicators. Land Degrad. Dev. 26, 843-852.

563 Schjønning, P., de Jonge, L.W., Munkholm, L.J., Moldrup, P., Christensen, B.T., Olesen, J.E.,

564   2012. Clay dispersibility and soil friability—Testing the soil clay-to-carbon saturation

565   concept. Vadose Zone J. 11, 174-187.

566 Scott, T., Macdonald, A.J., Goulding, K.W.T., 2014. The UK Environmental Change Network,

567   Rothamsted. Physical and Atmospheric Measurements: The First 20 Years. Lawes

568   Agricultural Trust Co. Ltd., Harpenden.

569 Six, J., Conant, R.T., Paul, E.A., Paustian, K., 2002. Stabilization mechanisms of soil organic

570   matter: Implications for C-saturation of soils. Plant Soil 241, 155-176.

571 Sohi, S.P., Mahieu, N., Arah, J.R.M., Powlson, D.S., Madari, B., Gaunt, J.L., 2001. A Procedure for

572   Isolating Soil Organic Matter Fractions Suitable for Modeling. Soil Sci. Soc. Am. J. 65,

573   1121-1128.

574 Stewart, C.E., Paustian, K., Conant, R.T., Plante, A.F., Six, J., 2007. Soil carbon saturation:

575   concept, evidence and evaluation. Biogeochemistry 86, 19-31.

576 Tisdall, J.M., Oades, J.M., 1982. Organic matter and water-stable aggregates in soils. J. Soil Sci.

577   33, 141-163.

578 Toms, J.D., Lesperance, M.L., 2003. Piecewise regression: A tool for identifying ecological

579   thresholds. Ecology 84, 2034-2041.

580 Villada, A., Vanguelova, E.I., Verhoef, A., Shaw, L.J., 2016. Effect of air-drying pre-treatment on

581   the characterization of forest soil carbon pools. Geoderma 265(Supplement C), 53-61.

582 Watts, C.W., Dexter, A.R., 1997. The influence of organic matter in reducing the destabilization of

583   soil by simulated tillage. Soil Tillage Res. 42, 253-275.

584 Weil, R.R., Islam, K.R., Stine, M.A., Gruver, J.B., Samson-Liebig, S.E., 2003. Estimating active

585   carbon for soil quality assessment: A simplified method for laboratory and field use. Am. J.

586   Alternative Agr. 18, 3-17.

587

588

Figure captions

590 **Fig. 1.** Distribution of plots in Highfield showing the arable (A), ley-arable (LA) and grass (G)

591 treatments in blocks 1-4 of the ley-arable experiment, and the bare fallow (BF) treatment in blocks

592 1-3 of the bare fallow experiments.

593 **Fig. 2.** (a) Permanganate oxidizable carbon (POXC) as a function of SOC and (b) hot water-

594 extractable carbon (HWC) as a function of SOC for the four treatments at subplot level. The

595 broken-stick and linear regression models are indicated.

596 **Fig. 3.** Principal component analysis (PCA) based on FTIR-PAS spectra for the different

597 treatments. The dots indicate the four plots of each treatment. For treatment abbreviations, see Fig.

598 1. (a) Scores plot in the plane defined by principal component 1 (PC1, explaining 84.6% of the

599 variance) and principal component 2 (PC2, explaining 7.5% of the variance) of the PCA. (b)

600 Loadings of the PCA for PC1 and PC2.

601 **Fig. 4.** Clay dispersibility of 1-2 mm aggregates rewetted to -100 hPa (solid lines) and

602 disintegration (the ratio between clay content estimated without SOM removal and with removal)

603 (dashed lines) as a function of (a) soil organic carbon (SOC), (b) permanganate oxidizable carbon

604 (POXC), and (c) hot water-extractable carbon (HWC) for the four treatments at subplot level. The

605 broken-stick models (Table 3) are indicated. See Table 3 for equations and R^2-values.

606 **Fig. 5.** (a) Clay dispersibility and (b) Clay-SOM disintegration as a function of soil organic carbon

607 (SOC; black symbols) and LF-free-SOC (Light fraction-free-SOC; white symbols). The broken-

608 stick models and R^2-values are indicated.

609 **Fig. 6.** (a) The ratio between dispersed particles <20 μm and the total content of particles <20 μm as

610 a function of Log10(min) at treatment level. The standard error of the mean is indicated (n=4). The

611 polynomials are fitted to the four replicates time's seven data points per treatment. Letters denote

612 statistical significance at $P<0.05$ for the comparison of A, LA and G. An asterisk (*) indicates if BF

613 is significantly different from A, LA and G based on a pairwise t-test. (b) Release rate (kg kg^{-1}

614 minerals dispersed min^{-1}) as a function of Log10(min) at treatment level. A stepwise, simple

615 calculation of slope from time step to time step was employed to calculate the release rate, and a

616 smoothed spline curve was added.

617

618   **Table 1** Soil characteristics. Within rows, letters denote statistical significance at $P<0.05$ for the

619   comparison of A, LA and G. An asterisk (*) indicates if BF is significantly different from A, LA

620   and G based on a pairwise t-test. For treatment abbreviations, see Fig. 1.

	BF	A	LA	G
Texture[a]				
Clay <2 µm	0.270	0.264	0.255	0.261
Silt 2-20 µm	0.249	0.263	0.261	0.272*
Silt 20-63 µm	0.335	0.318	0.324	0.319
Sand 63-2000 µm	0.146	0.155	0.160	0.148
Specific surface area (m^2 g^{-1} minerals)[b]	56.7	67.9^{a*}	68.4^{a*}	78.4^{b*}
Exchangeable cations and CEC				
Na^+ ($mmol_c$ kg^{-1} minerals)	0.4	0.5^a	0.4^a	0.7^{b*}
K^+ ($mmol_c$ kg^{-1} minerals)	3.3	6.3	17.7	5.8
Ca^{2+} ($mmol_c$ kg^{-1} minerals)	93.7	113.3^a	128.7^a	155.6^{b*}
Mg^{2+} ($mmol_c$ kg^{-1} minerals)	5.4	4.0	4.1	4.6
Sum of bases ($mmol_c$ kg^{-1} minerals)	102.9	107.1^a	120.7^{ab}	142.0^{b*}
CEC ($mmol_c$ kg^{-1} minerals)	145.8	173.8	171.3	209.9*
Base saturation (%)	72.8	65.5	74.8	74.4
pH ($CaCl_2$)	5.7	5.1	5.1	5.4

621   [a]kg kg^{-1} of mineral fraction and based on oven-dry weight.

622   [b]Clay is included as a co-variable since it is significant in itself and makes the treatment effect

623   significant.

624

625 **Table 2** Soil organic matter characteristics, clay dispersibility of 1-2 mm aggregates rewetted to -

626 100 hPa and clay-SOM disintegration (the ratio between clay content estimated without SOM

627 removal and with removal). Within rows, letters denote statistical significance at $P<0.05$ for the

628 comparison of A, LA and G. An asterisk (*) indicates if BF is significantly different from A, LA

629 and G based on a pairwise t-test. For treatment abbreviations, see Fig. 1.

|	BF	A	LA	G
Soil organic matter characteristics				
Soil organic carbon (SOC, kg kg^{-1} minerals)	0.0090	0.0173^{a*}	0.0216^{a*}	0.0329^{b*}
Permanganate oxidizable carbon (POXC, g kg^{-1} minerals)	0.161	0.458^{a*}	0.600^{b*}	0.818^{c*}
% of SOC	1.7	2.6^{ab*}	2.8^{b*}	2.5^{a*}
Hot water-extractable carbon (HWC, g kg^{-1} minerals)	0.437	0.777^{a*}	1.082^{b*}	1.611^{c*}
% of SOC	4.6	4.5^{a}	5.0^{b}	4.9^{ab}
Light fraction carbon (LFSOC, g kg^{-1} minerals)	0.167	1.285^{a*}	1.732^{a*}	2.579^{b*}
% of SOC	1.9	7.4*	8.0*	7.8*
Aliphatic peak area	58	99^{a*}	121^{a*}	159^{b*}
Aliphatic peak area/SOC	65	57	56	49*
Soil structural stability				
Clay dispersibility (DispClay, kg kg^{-1} minerals)	0.0115	0.0074^{c*}	0.0051^{b*}	0.0034^{a*}
Clay-SOM disintegration (DI, kg kg^{-1} minerals)	1.02	0.96^{b}	1.00^{b}	0.74^{a*}

630

631

632 **Table 3** Parameters of the linear, semi-logarithmic and broken-stick models for clay dispersibility (DispClay; kg kg^{-1} minerals) and clay-

633 SOM disintegration (DI; kg kg^{-1} minerals) as a function of soil organic carbon (SOC; kg kg^{-1} minerals), permanganate oxidizable carbon

634 (POXC; g kg^{-1} minerals), and hot water-extractable carbon (HWC; g kg^{-1} minerals). The change point of the broken-stick model and the

635 corresponding 95% confidence interval is indicated. The relation between the first and second slope estimate of the broken-stick model

636 (Slope1/Slope2) was calculated if both slopes were significant. The coefficient of determination (R^2) is indicated.

Predictor	Model		Equation	Change point	Slope1/Slope2	R^2
SOC	Linear	DispClay	0.0134*** -0.32*** SOC			0.839
		DI	1.16*** -11.6*** SOC			0.723
	Semi-log	DispClay	-0.0189*** -0.0148*** log(SOC)			0.930
		DI	0.16*** -0.442*** log(SOC)			0.555
	Broken-stick	DispClay	0.0160*** -0.49*** SOC + 0.39*** (SOC-0.0235)$^+$	0.0235*** [0.0209:0.0260]	4.6	0.940
		DI	1.03*** -2.9^{NS} SOC – 18.0*** (SOC-0.0225)$^+$	0.0225*** [0.0199:0.0251]		0.880
POXC	Linear	DispClay	0.0131*** -0.0122*** POXC			0.907
		Di	1.11*** -0.366*** POXC			0.550
	Semi-log	DispClay	0.0029*** -0.011*** log(POXC)			0.891
		DI	0.83*** -0.261*** log(POXC)			0.364
	Broken-stick	DispClay	0.0136*** -0.0138*** POXC + 0.0084* (POXC-0.694)$^+$	0.694* [0.564:0.824]	2.6	0.927
		DI	1.02*** -0.087^{NS} POXC - 1.00*** (POXC-0.628)$^+$	0.628*** [0.573:0.683]		0.819
HWC	Linear	DispClay	0.0128*** -0.0061*** HWC			0.815
		DI	1.13*** -0.21*** HWC			0.648
	Semi-log	DispClay	0.0059*** -0.0133*** log(HWC)			0.900
		DI	0.90*** -0.378*** log(HWC)			0.490
	Broken-stick	DispClay	0.0156*** -0.0105*** HWC + 0.00760*** (HWC-0.970)$^+$	0.970*** [0.833:1.107]	3.6	0.913
		DI	1.02*** -0.049^{NS} HWC – 0.341*** (HWC-1.104)$^+$	1.104*** [0.921:1.288]		0.788

637   * and *** indicate significance level at $P<0.05$ and $P<0.001$, respectively.
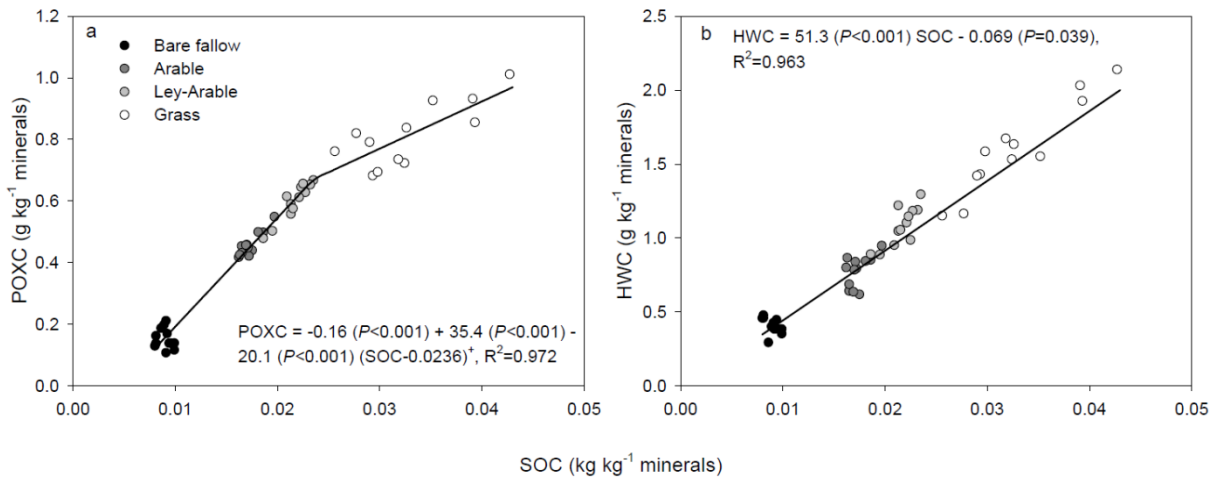
638   NS: Not significant.

639    $^+$: Indicates that the last term is valid only when the content of SOC, POXC or HWC are larger than the change point.
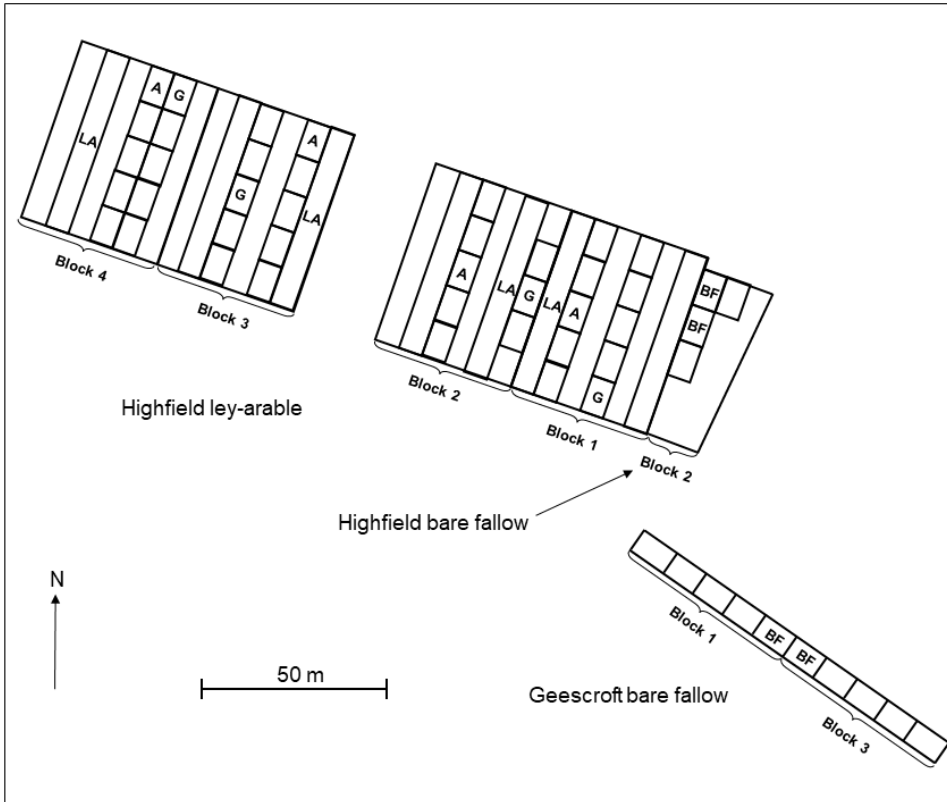
640

Fig. 1. Distribution of plots in Highfield showing the arable (A), ley-arable (LA) and grass (G)

treatments in blocks 1-4 of the ley-arable experiment, and the bare fallow (BF) treatment in blocks
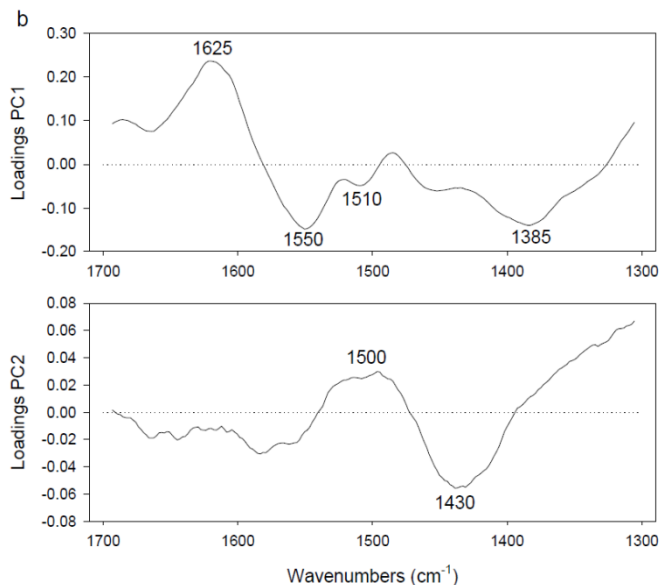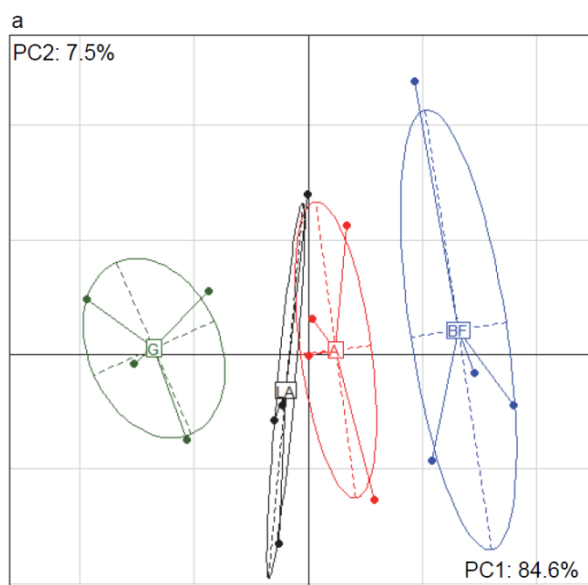
1-3 of the bare fallow experiments.

644

645

646 **Fig. 2.** (a) Permanganate oxidizable carbon (POXC) as a function of SOC and (b) hot water-

647 extractable carbon (HWC) as a function of SOC for the four treatments at subplot level. The

648 broken-stick and linear regression models are indicated.

649

Fig. 3. Principal component analysis (PCA) based on FTIR-PAS spectra for the different treatments. The dots indicate the four plots of each treatment. For treatment abbreviations, see Fig. 1. (a) Scores plot in the plane defined by principal component 1 (PC1, explaining 84.6% of the variance) and principal component 2 (PC2, explaining 7.5% of the variance) of the PCA. (b) Loadings of the PCA for PC1 and PC2.
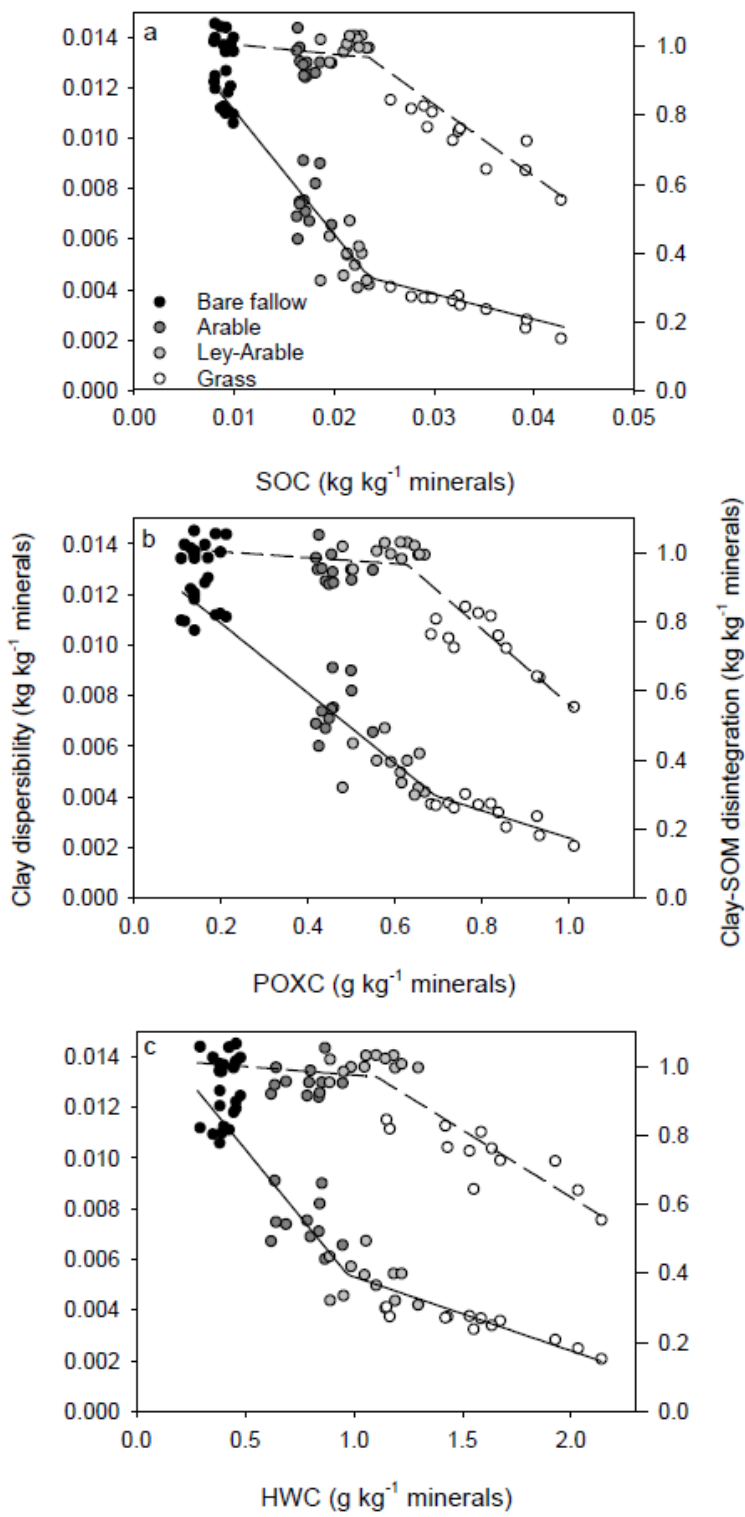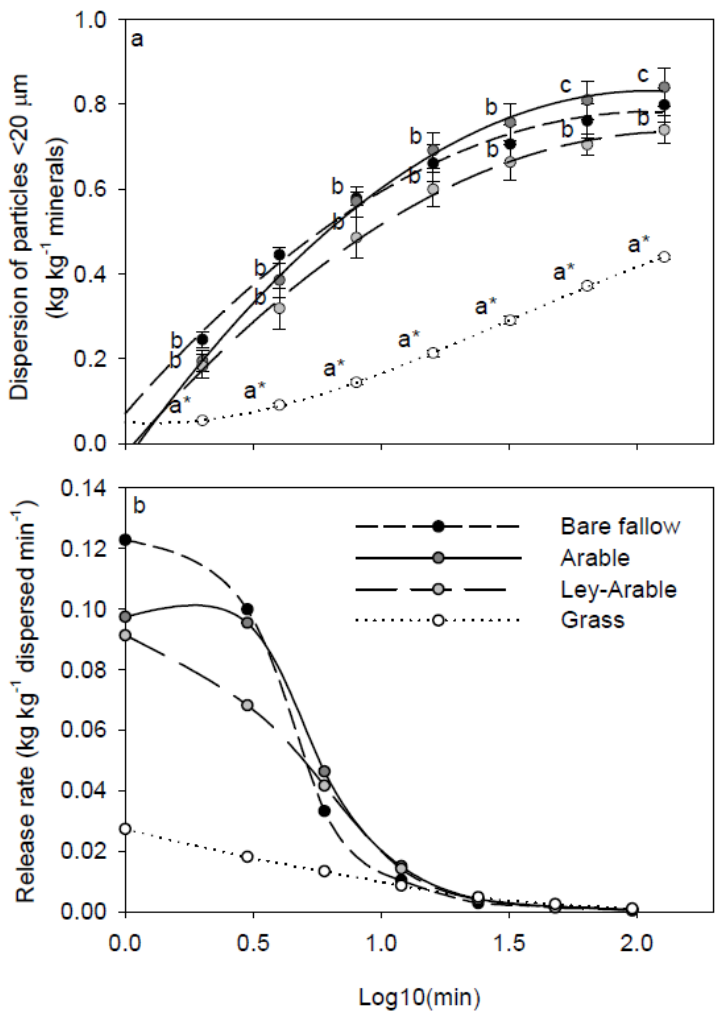
657

658

659 **Fig. 4.** Clay dispersibility of 1-2 mm aggregates rewetted to -100 hPa (solid lines) and clay-SOM

660 disintegration (the ratio between clay content estimated without SOM removal and with removal)

661 (dashed lines) as a function of (a) soil organic carbon (SOC), (b) permanganate oxidizable carbon

662 (POXC), and (c) hot water-extractable carbon (HWC) for the four treatments at subplot level. The

663 broken-stick models (Table 3) are indicated. See Table 3 for equations and R^2-values.

664

665
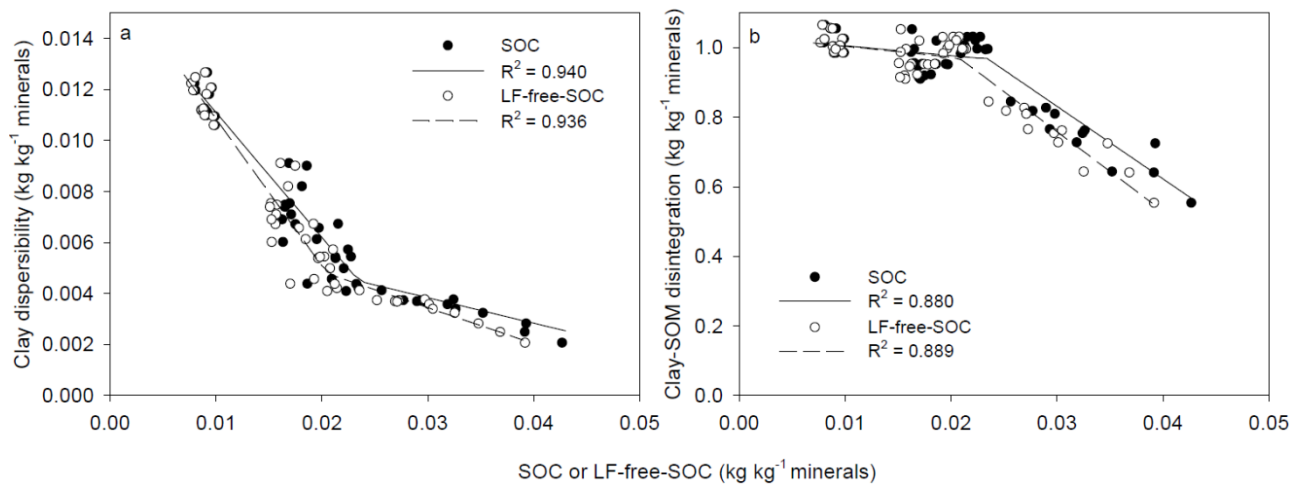
Fig. 5. (a) Clay dispersibility of 1-2 mm aggregates rewetted to -100 hPa and (b) Clay-SOM

disintegration (the ratio between clay content estimated without SOM removal and with removal) as

a function of soil organic carbon (SOC; black symbols) and LF-free-SOC (Light fraction-free-SOC;

white symbols). The broken-stick models and R^2-values are indicated.

670

671

Fig. 6. (a) The ratio between dispersed particles <20 μm and the total content of particles <20 μm as a function of Log10(min) at treatment level. The standard error of the mean is indicated (*n*=4). The polynomials are fitted to the four replicates time's seven data points per treatment. Letters denote statistical significance at *P*<0.05 for the comparison of A, LA and G. An asterisk (*) indicates if BF is significantly different from A, LA and G based on a pairwise *t*-test. (b) Release rate (kg kg^{-1} minerals dispersed min^{-1}) as a function of Log10(min) at treatment level. A stepwise, simple calculation of slope from time step to time step was employed to calculate the release rate, and a smoothed spline curve was added.

40

Supplementary material for the article entitled: "Relating soil C and organic matter fractions to structural stability" by Jensen et al.
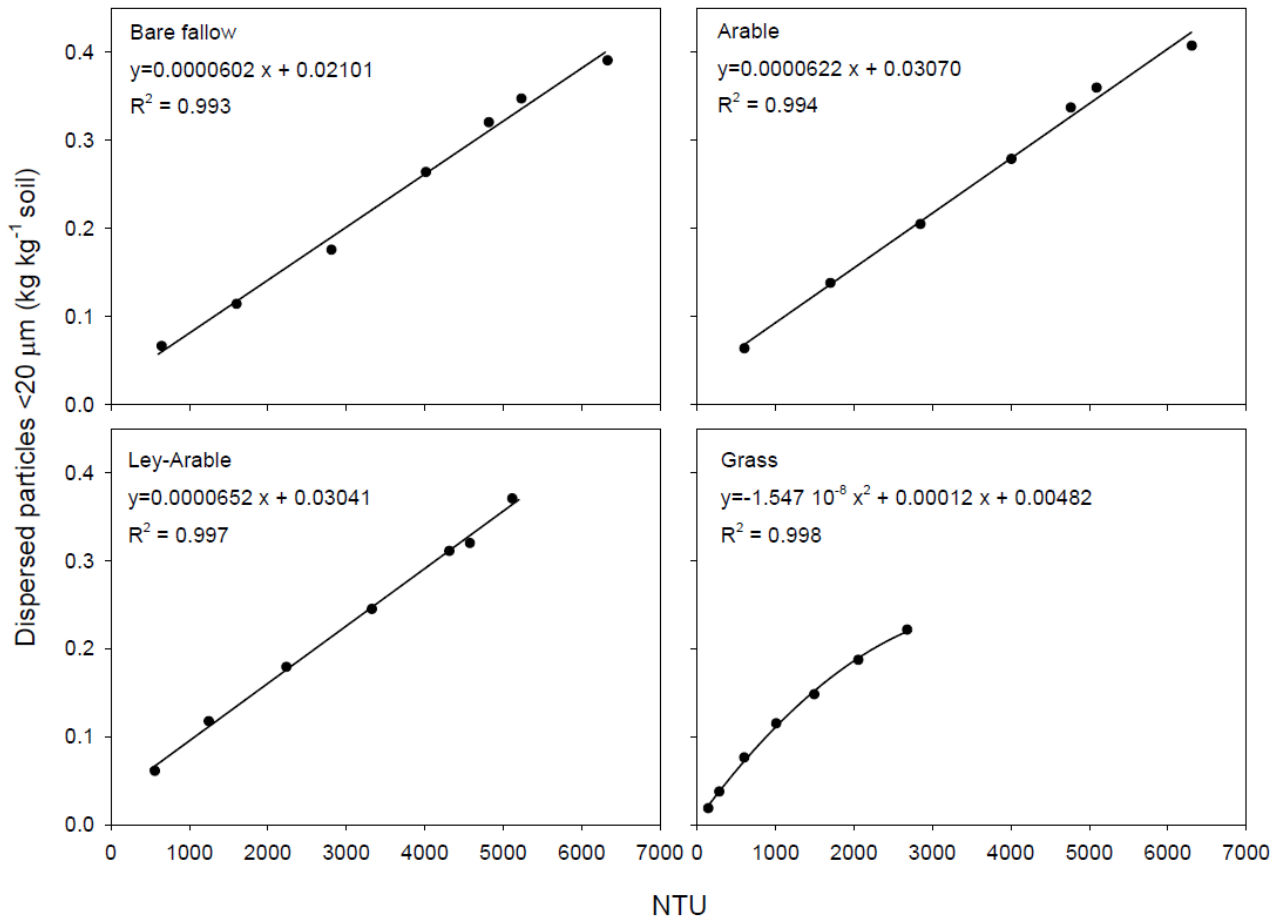

Fig. S1. The correlation between nephelometric turbidity (NTU) and dispersed particles <20 μm (kg kg^{-1} soil) for the four different treatments.
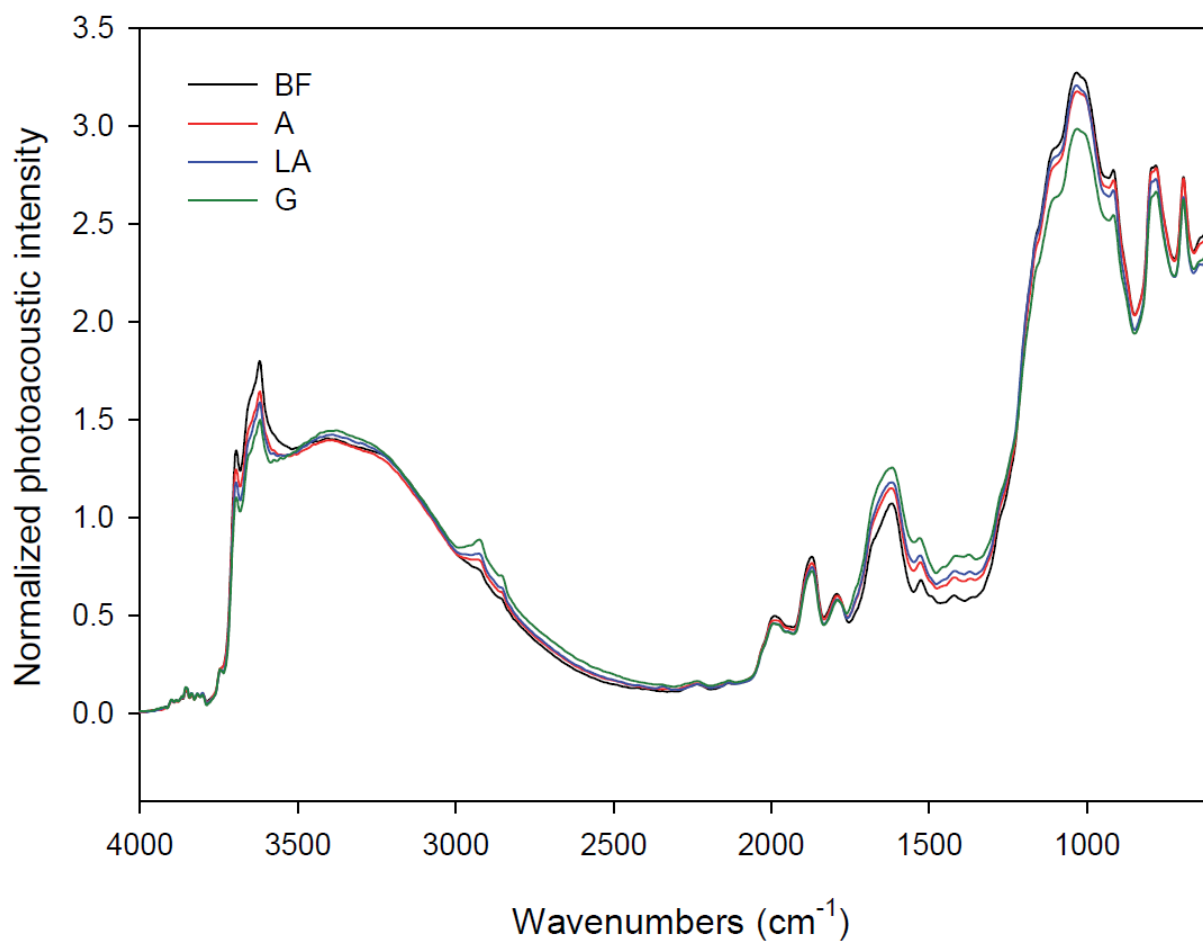
Fig. S2. Spectra of the different treatments from Highfield over the selected FTIR region 4000-600 cm^{-1}. The spectra are presented as the average of the spectra from the four field plots. BF, Bare fallow; A, Arable; LA, Ley-arable; G, Grass.
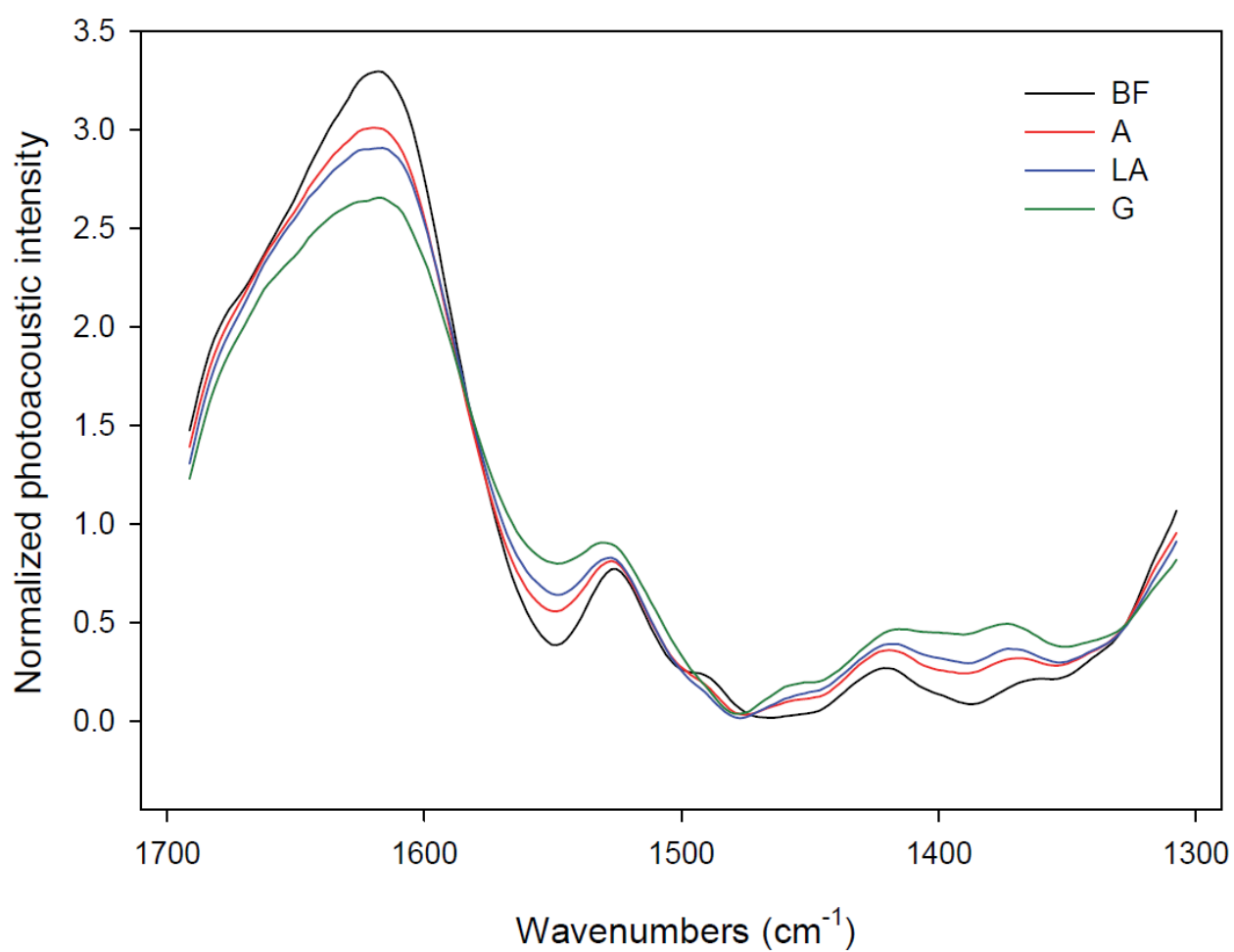
Fig. S3. Spectra of the different treatments from Highfield over the selected FTIR region 1700-1300 cm^{-1}. The spectra are presented as the average of the spectra from the four field plots. BF, Bare fallow; A, Arable; LA, Ley-arable; G, Grass.
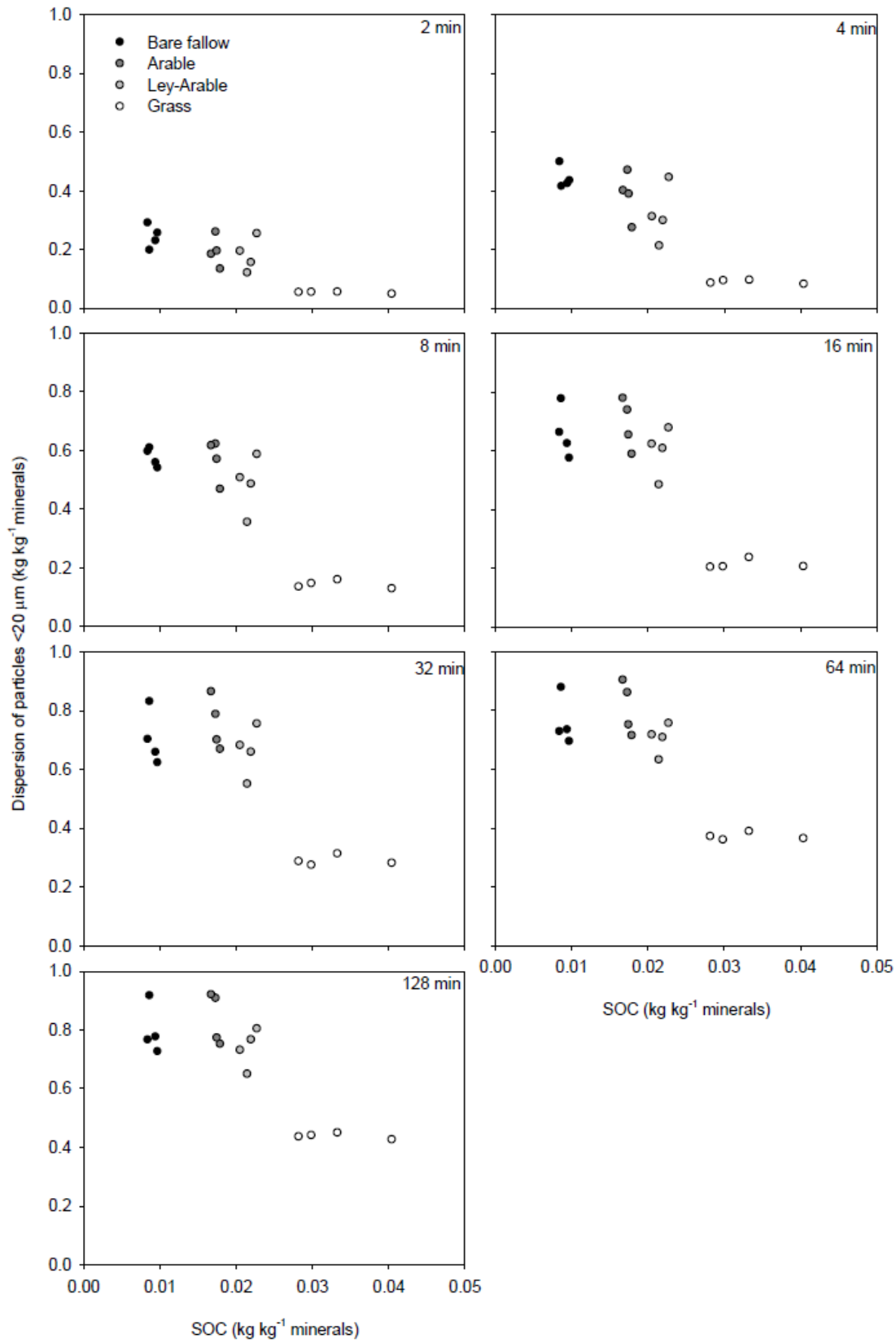
Fig. S4. The ratio between dispersed particles <20 μm and the total content of particles <20 μm as a function of soil organic carbon at plot level for the seven time steps.